

TECHNICAL PAPER

Co-Registration of Cardiac MRI and Rest Gated SPECT in the Assessment of Myocardial Perfusion, Function and Viability

Jolanta Misko,¹ Mirosław Dziuk,² Ewa Skrobowska,³ Norbert Szalus,⁴ Jacek Pietrzykowski,⁴
and Agnieszka Warczynska³

Department of Nuclear Medicine, Central Rail Hospital, Warsaw, Poland,¹ Departments of Internal Medicine and Cardiology,² Department of Radiology,³ Department of Nuclear Medicine,⁴ Military Institute of Health Services, Warsaw, Poland

ABSTRACT

Purpose: Myocardial perfusion is routinely measured by SPECT—this technique has a rather low spatial resolution but covers the whole myocardium and is equipped with efficient image analysis software. Cardiac MRI has higher spatial resolution than SPECT and excellent sequences for myocardial function and viability detection but the lack of easy-to-use methods of acquisition and post-processing of perfusion images prevents this method from being used for perfusion evaluation in clinical practice. The aim of the study was to explore whether the 3-D co-registration of “cine” MRI (cine MRI), delayed enhancement MRI (DE MRI) and gated SPECT (GSPECT) images might be used for differentiating all reversible and irreversible effects of ischemia in anatomically matched myocardial regions. **Methods:** We analyzed 685 segments of the heart (6 segments in each short axis slice)—obtained as a result of MRI and GSPECT studies performed in 18 patients. In each segment, myocardial function, perfusion and viability were analyzed. Myocardial wall function was evaluated using the matched images of diastolic and systolic phases of cine MRI. Perfusion as MIBI uptake per volume (MIV) (counts/mm³) in each myocardial segment was evaluated by co-registration of diastolic phases of cine MRI and GSPECT. Transmural extent of infarction was determined by co-registration of DE MRI and diastolic phase of cine MRI. **Results:** We have found a close correlation between regional perfusion and function at rest in matched MRI and SPECT images: dysfunctional segments had significantly less MIV (MIV = 4.63 SD 1.58) than normal segments (MIV = 8.86 SD 2.77) ($p < .05$). There was no significant difference in MIV between viable and non-viable dysfunctional segments defined by DE MR due to a small number of nonviable segments in our study (18/685). **Conclusion:** Matching rest perfusion and function in anatomically co-registered myocardial segments in our study confirms that 3-D image co-registration of cine MRI, DE MRI and gated SPECT could be a precise method of integrated visualization of perfusion, function and viability helping in differentiating all forms of reversible and irreversible effects of myocardial ischemia.

Keywords: Cardiac MRI, SPECT, Image Fusion, Myocardial Viability, Myocardial Perfusion, Myocardial Function

Correspondence to:

Jolanta Misko

Department of Nuclear Medicine

Central Rail Hospital

ul. Bursztynowa 2

04-479 Warsaw, Poland

phone: (48 22) 513 51 96 fax: (48 22) 815 67 39

email: jmisko@wp.pl

INTRODUCTION

Coronary artery disease (CAD) is one of the main causes of mortality and disability nowadays. Insufficient coronary blood flow with reduced myocardial perfusion often leads to the left ventricular dysfunction (1). Patients with CAD and left ventricular dysfunction not only have a poor survival rate, but the risk of acute cardiac events is higher than in others because the myocardium supplied by an affected artery is at risk of ischemia and injury (2–6). About 25–40% of patients with CAD and reduced

left ventricular ejection fraction could improve myocardial function following successful revascularization (2, 5, 7–9) because they have ischemic but still viable myocardium (hibernating myocardium) in the dysfunctional region (1, 10–13). There is also another group of CAD patients who have no myocardial dysfunction but are at higher risk of acute cardiac events. Those patients have myocardium at risk detectable as reversible perfusion defects or decreased coronary flow reserve in stress-rest perfusion studies (4).

The main goal of clinical cardiac imaging techniques is to identify myocardial viability and myocardium at risk (2, 3, 11–15) because patients with dysfunctional but viable myocardium and patients with myocardium at risk are the only ones who benefit from revascularization procedures since non-viable segments do not benefit from revascularization. Patients with hibernating myocardium treated medically had worse prognosis than those who underwent revascularization (2, 5).

Each of noninvasive methods of cardiac imaging, echocardiography, SPECT, MRI, PET, and CT, has its advantages and disadvantages in depicting myocardial function, perfusion and viability, and, until now, none of them can be a diagnostic “one-stop-shop.”

Previous studies have demonstrated that cine MRI is treated as a gold standard in imaging cardiac morphology and function and has higher spatial resolution than PET or SPECT in viability imaging (15–17). Transmural extent of hyperenhancement is used to predict an improvement of myocardial function (18–27). Regions with transmural extension of hyperenhancement greater than 50% are less likely to improve wall motion (17, 18, 23–25).

Cardiac MRI is not as widely used as SPECT. The SPECT perfusion study is an established procedure used for diagnosing myocardial perfusion and viability, but it may miss small or subendocardial necrosis due to its spatial resolution comparable to myocardial wall thickness (27–31). On the other hand, perfusion SPECT produces sum up 3-D images of stress and rest myocardial perfusion covering the whole left ventricle myocardium and with higher signal to background contrast in comparison to perfusion MRI. Additionally, in its acquisition and analysis, perfusion MRI misses a very important part of the apical region of the myocardium.

3-D fusion by the use of specific software to combine functional and structural imaging in cardiology could be a solution for precise, high accuracy diagnostics of all hemodynamically significant effects of ischemia in the myocardium supplied by an affected coronary artery.

The aim of the study was to explore a potential role of 3-D co-registration of cine MRI, delayed enhancement MRI and rest gated SPECT (GSPECT) with technetium-99 m Sestamibi in the comprehensive evaluation of all reversible and irreversible forms of myocardial ischemia by investigating a correlation between perfusion, function and viability in precisely defined, anatomically matched myocardial segments in patients with CAD.

METHODS

Patient population

We investigated 18 patients (pts) (12 males, 6 females, mean age 67.6 years, range 53–82) with stable coronary artery disease (CAD) after acute coronary events: 8 patients with myocardial infarction (MI) and 10 pts with suspected MI. This study was approved by the Institutional Review Board of Military Institute of Health Sciences in Warsaw. All the patients gave their informed consent.

All patients were subjected to cine MRI, DE MRI study and rest GSPECT study within 3 days from the onset of symptoms. Patients were included if they had: (1) regular heart rate, (2) circulatory and respiratory stabilization, or (3) no contraindications to MRI. No patient had clinical evidence of a new myocardial infarction between MRI and GSPECT scans.

Imaging protocols

MR imaging

All patients underwent MR imaging with a 1.5-T scanner (GE, Milwaukee, WI, USA, Signa Horizon Echo Speed Plus) equipped with cardiac software package. Images were acquired during repeated breath-holds, all images were ECG gated. Cine MRI was performed using a steady state free precession sequence FIESTA (TR/TE = 4/1.8 ms; FOV 400 × 360 mm; slice thickness—8 mm; 256 × 256 matrix; acquisition over 15–23 heart beats) in following orientations: 2-chamber long axis, 4-chamber long axis, and short axis covering the entirety of the left ventricle. DE MR images were acquired using a segmented inversion recovery gradient echo pulse sequence (TR/TE/TI = 8/4/200–300 ms; field of view of 400 × 360 mm; slice thickness 8 mm) 10–20 minutes after contrast administration (0.15 mmol/kg gadolinium) in the same orientations as in cine-MRI. Both cine and DE images were arranged every 8 mm from base to apex (6–8 short axis slices). In the image plane, the resolution was 1.64 × 1.64 mm.

GSPECT imaging

Rest gated ECG SPECT (GSPECT) was performed within 72 hours after cardiac MRI. GSPECT was acquired 45–60 minutes after intravenous administration of 925 MBq of Sestamibi Tc99m (MIBI) with a dual-detector gamma camera (Elsint, Haifa, Israel, Varicam), with 60 projections each for 25 seconds with a circular 180 degree orbit. A low-energy, high-resolution collimator was used with a 20% window. No attenuation correction was used. The data were processed with an Xpert software. After a filtered back-projection reconstruction, short axis tomograms from diastolic phase were generated. Images were reconstructed with Butterworth filter (cut-off 0.35, order 5). Voxel size was isotropic in 3 directions—6.4 mm.

Image co-registration

For image co-registration two types of software, PMOD (PMOD Technologies, Zurich, Switzerland) image fusion tool

(PFUS) and HERMES (HEMES Medical Solutions, Stockholm, Sweden) Nuclear Diagnostics (Multimodality), were used. Programs allow for the manual realignment of volumetric image sets and are equipped with tools for pixel-wise image algebra on registered images and volume-of-interest definition directly in the co-registered image display. Original cine MR and DE MR images were transferred to workstations in DICOM format. Reconstructed SPECT images were transferred in Interfile format. In all end-diastolic SPECT images the maximum count number in voxel was normalized to the same value using image algebra tool in PFUS. In the process of co-registration, images belong to two categories—one set with higher resolution served as reference (MRI), and the other set with lower resolution was regarded as reslice (SPECT). Both sets were resampled to the same resolution as the reference by the interpolation of SPECT matrix (64×64) to the MRI matrix (256×256). Matching cine MR, DE MR and GSPECT images required the reslice images to be rotated and shifted manually in all three dimensions of the orthogonal planes until they got into a spatial alignment with the reference. In order to obtain a precise manual co-registration, we used the following anatomic landmarks: right ventricle insertions, papillary muscles, and the shape of the left and right ventricles. Two independent observers needed about 20 minutes to perform a manual co-registration of cine MRI or DE MRI and GSPECT images and about 5–10 minutes to perform cine MR and DE MR image co-registration. Each set of combined short axis images contained 6–8 slices similar to those received in the reference MR imaging of the heart.

Data analysis

Co-registered MRI and GSPECT short axis images were used in the analysis. Short axis slices located apically, difficult to visualize in the MRI, were excluded from the analysis. The segments adjoining the left ventricular outflow track were also excluded. All matched short axis images were divided into 6 radical segments: anteroseptal, anterior, anterolateral, inferolateral, inferior and inferoseptal (Fig. 1a, 1b). Thus, in total, myocardial function, perfusion, and viability were analyzed in 685 myocardial segments.

Myocardial function

The myocardial function evaluation was performed in automatically co-registered end-diastolic and end-systolic cine MR images. The inversion grey color scale on end-diastolic images and narrow color windows for both sets of images were applied. In the segments with normally contracting myocardium, combined images showed a dark rim between the endocardial border during diastolic and systolic phases (Fig. 2). The rim was narrow in the hypokinetic segment and invisible in the akinetic one. We measured the distance between diastolic and systolic borders and the thickness of myocardial wall during end-diastole and end-systole. We divided the regional myocardial function of each segment into two types:

- normal function (normokinetic) with a difference between systolic and diastolic borderline equal or more than 3 mm—**group A**,

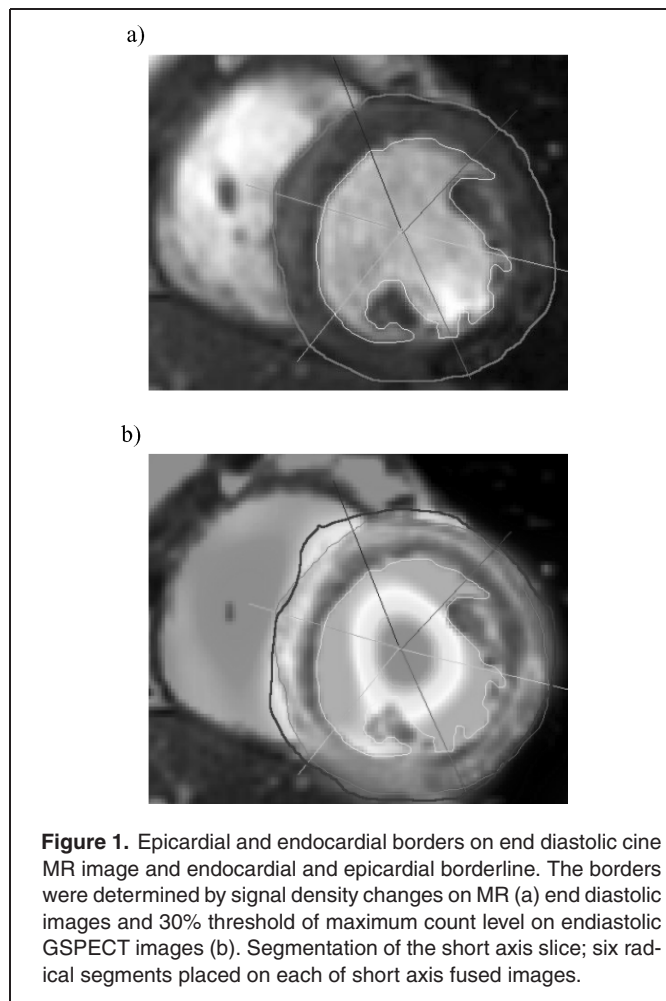


Figure 1. Epicardial and endocardial borders on end diastolic cine MR image and endocardial and epicardial borderline. The borders were determined by signal density changes on MR (a) end diastolic images and 30% threshold of maximum count level on end-diastolic GSPECT images (b). Segmentation of the short axis slice; six radical segments placed on each of short axis fused images.

- abnormal function (dysfunctional) with a difference between systolic and diastolic borderline less than 3 mm—**group B**.

Myocardial perfusion

In order to analyze myocardial perfusion, end-diastolic cine MR short axis images and end-diastolic GSPECT short axis images were co-registered. In matched images, volumes-of-interest (VOIs) were defined using VOI constructor program (PFUS). All VOIs were defined in the layout showing each single short axis slice according to the localization of six radical segmentations (in all segments the distance in z-orientation was 8 mm due to the original z-distance of MRI study). In each segment, we manually delineated epicardial and endocardial borders on an end-diastolic cine MR image and endocardial and epicardial borderlines on end-diastolic GSPECT. The borders were determined by signal density changes on MR end-diastolic images (Fig. 1a), and a 30% threshold of maximum count level on end-diastolic SPECT images as an automatically defined isocontour line (Fig. 1b). We cannot use the same epicardial and endocardial borders on MR and SPECT images due to the partial volume effect on SPECT images. The statistical analysis program

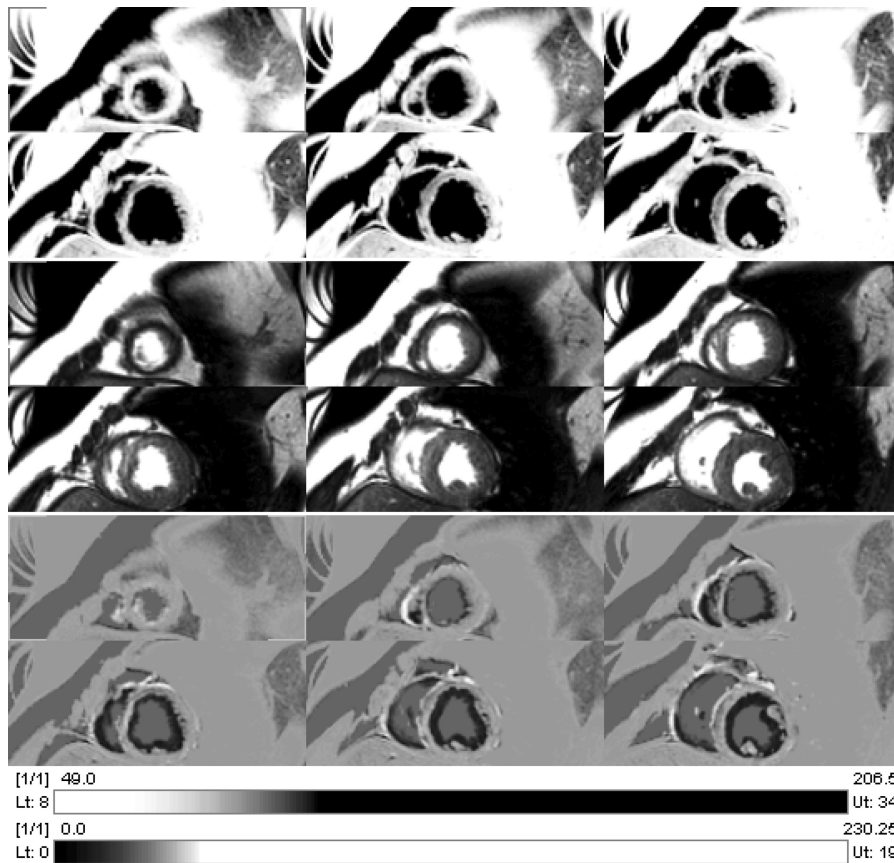


Figure 2. Fusion of end diastolic and end systolic cine MR images for myocardial function evaluation. Inversion grey color scale on end diastolic and narrow color window on both sets of images were applied. Dark rim on fused images represents distance between endocardial borderline during systolic and diastolic phases.

coupled with the VOI constructor allowed the volume and number of counts to be calculated in each myocardial segment. The number of counts divided by the volume (in mm^3) produced a new perfusion parameter in each segment: MIBI uptake density in volume—MIV ($\text{counts}/\text{mm}^3$).

Myocardial viability

The extent of an infarct was measured with DE MRI and cine MRI. To assess myocardial viability combined end-diastolic cine MR and DE MR images were used (Fig 3). In each segment of used images, we analyzed the transmural extension of myocardial necrosis using a “VOI constructor” by the manual delineation of the delayed enhancement volume compared to the volume obtained from cine images. We divided all myocardial segments into:

- Viable myocardium—segments without delayed enhancement (without necrosis)—**group X**;
- Viable myocardium with subendocardial necrosis—segments with delayed enhancement below 50% of segmental volume—**group Y**;
- Nonviable myocardium—segments with delayed enhancement above 50% of segmental volume—**group Z**.

Statistical analysis

The statistical analysis was performed using the CSS Statistica 5.1 PL program (StatSoft, Tulsa, USA). Continuous data were expressed as mean (\pm) SD. The Shapiro-Wilk and Mann-Whitney tests were used to assess the relationship between myocardial contractility, transmural extent of infarction and MIV perfusion index in all segments of the left ventricle. All statistical tests were two-tailed. The $p < .05$ value was regarded as statistically significant.

RESULTS

All 685 myocardial segments were divided into three groups according to the presence and extension of delayed enhancement defined by DE MRI (Table 1).

Table 1. Segmental analysis

| Groups of segments | A (normokinetic) | B (hypokinetic) | Summary |
|-------------------------|------------------|-----------------|---------|
| X (without enhancement) | 411 | 185 | 596 |
| Y (enhancement <50%) | 26 | 45 | 71 |
| Z (enhancement >50%) | 0 | 18 | 18 |
| Summary | 437 | 248 | 685 |

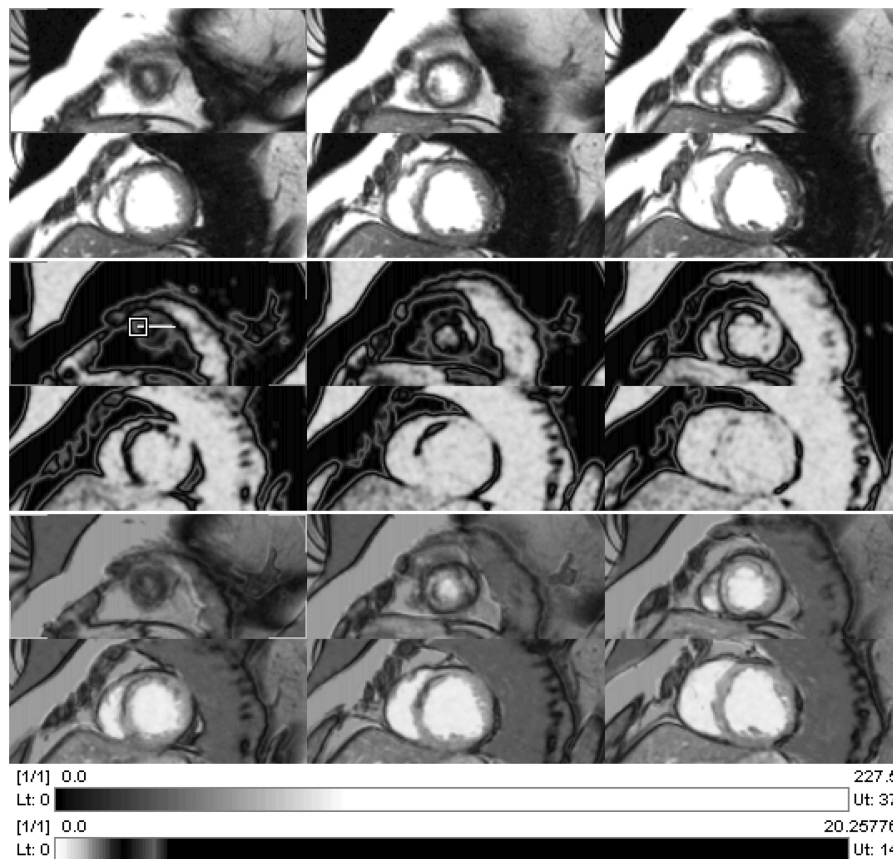


Figure 3. Fusion of end diastolic cine MR and DE MR short axis images for evaluation of various transmural extension of delayed enhancement—transmural extension of delayed enhancement of the antero-septal wall.

- 596 segments without delayed enhancement (viable),
- 71 segments with subendocardial necrosis below 50% of segmental volume (viable),
- 18 segments with necrosis above 50% of segmental volume (nonviable).

In the first two groups of myocardial segments (without enhancement and with enhancement below 50%), we found segments with normal and abnormal functions and differences in perfusion index MIV.

In 71 segments with subendocardial necrosis below 50% of segmental volume, we found that hypokinesis had occurred in 45 segments (63%). The remaining 26 segments (37%) were normokinetic. There was a difference in perfusion index MIV between hypokinetic and normokinetic segments in this group: dysfunctional segments had significantly less MIV than segments with normal function ($p < 0.05$) (Fig. 4a).

The same relationship was observed in a group of segments without delayed enhancement—185 (31%) segments in this group presented decreased wall motion and corresponding significant lower level of perfusion index MIV in comparison to the level of MIV in segments with normal function ($n = 411$).

In our study all segments with delayed enhancement above 50% of segmental volume (nonviable) were dysfunctional with

the level of perfusion index MIV similar to that found in all hypokinetic segments (Fig. 4a).

There were no statistically significant differences in MIV between normokinetic segments ($n = 437$) regardless of their localization in the different walls of the myocardium (Fig. 4b), regions of coronary blood supply (Fig. 4c), and the presence or absence of subendocardial necrosis below 50% of segmental volume (Fig. 4a).

We found significant differences in perfusion index MIV between normokinetic ($n = 437$) and hypokinetic ($n = 248$) segments (Fig. 5). Dysfunctional segments had significantly less MIV ($MIV = 4.63$ SD 1.58) than normal segments ($MIV = 8.86$ SD 2.77) ($p < 0.05$). The differences in MIV between normokinetic and hypokinetic segments were statistically significantly independent of the localization and amount of the myocardium with delayed enhancement.

There was no significant difference in MIV between viable and non-viable dysfunctional segments defined by DE MR (Fig. 4a).

DISCUSSION

As far as we know, this is the first study related to a potential clinical usefulness of the co-registration of images acquired

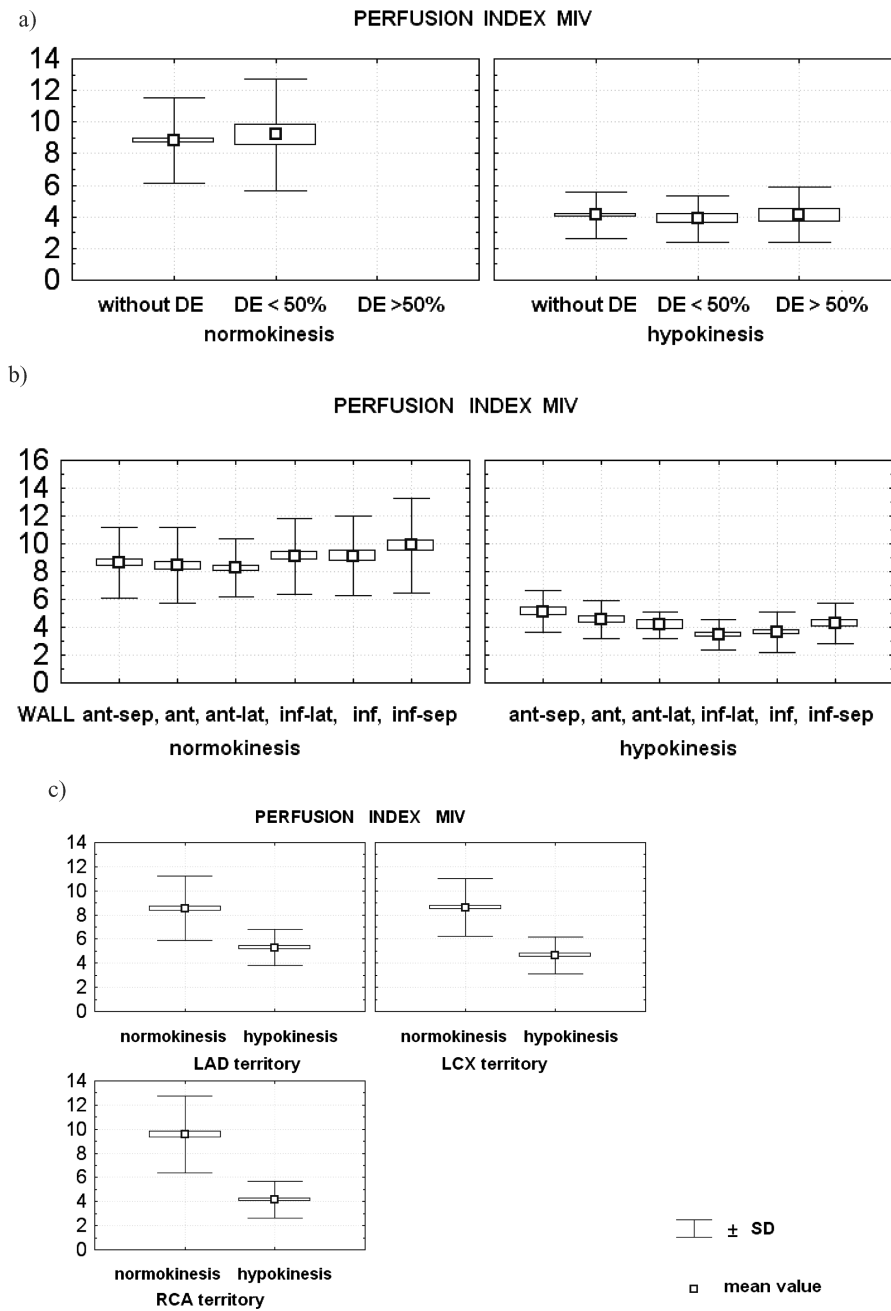
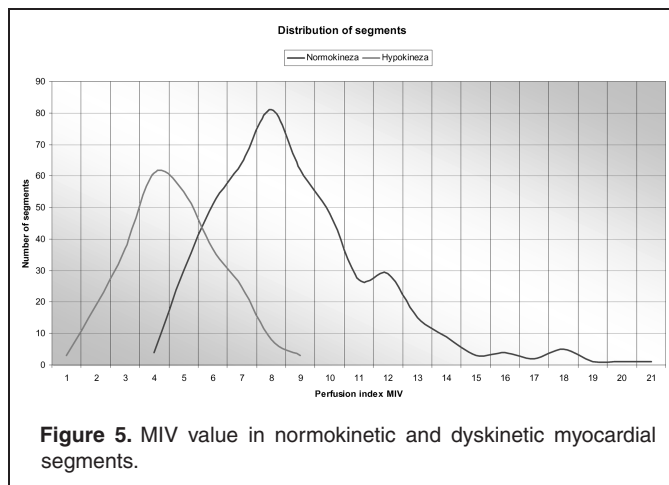


Figure 4. Perfusion index MIV in regions with different transmural extension of delayed enhancement (a), in myocardial walls (b) and in coronary artery territories (c) in areas with normokinesis and hypokinesis of myocardial walls.

from cardiac cine MRI, DE MRI, and GSPECT for obtaining comprehensive information about myocardial function, perfusion and viability.

The original concept of perfusion index in myocardial volume, MIV, is new and until now not used in cardiology. MIV requires the cine MR (or another type of cardiac anatomy imaging) and SPECT image co-registration. Naturally, MIV does not evaluate the absolute value of perfusion in tissue, but it takes into account the thickness or volume of a segment which influences the count rates. In an ischemic segment, there should be fewer

counts per segment than in a normal one (4). MIV in our study served as a quantitative parameter helping to assess the perfusion in tissue volume. We used it to compare the regional myocardial perfusion and function in order to verify the quality of matching in anatomically co-registered cine MRI and SPECT images. The mechanism of myocardial perfusion-contraction matching was described by Ross (32). The regional dysfunction observed in hibernation has been believed to be due to a reduction in resting blood flow to the myocardium (1, 7, 10). Thus, flow and function in the ischemic but viable myocardium are coupled in a parallel



manner: reduction in flow results in a reduction in function (32). In our study, a regional concentration of radioactivity in the corresponding volume of the myocardium was closely correlated with the regional myocardial function so we can treat 3-D co-registration of morphologic and functional cardiac images as a basis for the integration of information from various imaging modalities.

Our study results showed the composite character of ischemic patterns: wall motion abnormalities, perfusion abnormalities, and necrotic changes in the myocardium. In our study, 31% of segments without necrosis detected by DE MRI presented wall motion abnormalities and lower perfusion index MIV most probably caused by myocardial ischemia at rest (hibernation). In segments with limited subendocardial infarction on delayed enhancement gadolinium imaging, 63% of segments had dysfunction and lower level of MIV. Both these groups of segments could be defined as hypokinetic or hypoperfused using only one of morphologic (echocardiography, MRI) or metabolic (SPECT or PET) methods (33, 34). However, the remaining 37% of segments with a subendocardial infarction below 50% of wall extension presented normal contraction, and a well preserved rest perfusion could be diagnosed as ischemic only by DE MRI. SPECT was able to define each myocardial segment as viable or nonviable with high probability but could not detect small, subendocardial infarcts (27). This result suggests that the contractility of the myocardial wall in the region of subendocardial infarction is related to the perfusion level of the remaining viable tissue rather than to the necrotic layer. In a myocardial region consisting of a mixture of viable and necrotic tissue, we should measure perfusion in the residual myocardium. We can also suggest that there could be hidden segments with ischemia induced at stress (myocardium at risk) in a group of segments with normal function and normal perfusion, with or without limited subendocardial necrosis.

This finding does not change the prediction of functional recovery in the regions with subendocardial infarction and dysfunction. Yet, in patients with normal function and subendocardial infarction, a future analysis could be performed using a 3-D image co-registration of stress SPECT images instead of rest

SPECT images and cine MRI to identify myocardium at risk in the epicardial region (35, 36).

There was a fairly high number of dysfunctional segments without delayed enhancement in our study (75% of all dysfunctional segments). The explanation of this could be that all MRI and SPECT studies were performed 3 days after the onset of acute cardiac events without prior revascularization so our patients could develop all stages of stunning, ongoing ischemia, “threshold phenomenon,” and tethering described in the situation of acute infarction.

In our study we also introduced some new methods of determining the infarct extent and transmural in co-registered images from DE MRI and cine MR and myocardial function in co-registered diastolic and systolic images from cine MRI.

A close correlation between the perfusion and function in matched myocardial segments from rest SPECT and cine MR images presented in our study may suggest that co-registration of stress SPECT, cine MRI, and DE MRI can be helpful in the evaluation of even subtle stress perfusion abnormalities, subendocardial, small necrosis and discreet functional abnormalities in the area of the myocardium supplied by an affected coronary artery (36).

Identification of even small myocardial infarcts is prognostically important because each MI is associated with poorer prognosis (34, 37, 38). Previous studies have shown that the transmural extent of hyperenhancement by contrast-enhanced MRI corresponds to the transmural extent of infarction (27, 39). DE MRI does not require exercise or pharmacological stress testing and, unlike other existing techniques, allows for a direct visualization of the necrotic tissue. In our study, MRI was well tolerated and images obtained were of high quality (14).

Our results might have been biased due to a small number of non-viable full thickness infarctions. Other limitations of this paper included a relatively small patient population and possible mistakes during the discrimination between normal and dysfunctional segments. The results of our study suggest the need for further research in larger patient population and after stress in order to determine the segmental coronary flow reserve.

CONCLUSION

3-D image co-registration of cardiac MRI and rest gated SPECT allows precise matching of perfusion and function in myocardial segments to be obtained and could be a new and promising diagnostic tool in the integration of information from various imaging modalities: SPECT, PET, MRI and CT.

Basing on the concordance between rest perfusion and function in our study, we can conclude that co-registration of different images of the heart can be performed to better characterize cardiac anatomy, function, viability and perfusion at stress in myocardial segments.

ACKNOWLEDGMENTS

This work was supported by a grant from Polish Scientific Committee No 3 PO5B 094 24 and by cooperation with

HERMES Nuclear Diagnostics. We thank Professor Eugeniusz Dziuk, MD, PhD; Professor Marian Cholewa, MD, PhD; Professor Jerzy Adamus, MD, PhD; Professor Leszek Kubik MD, PhD; and Piotr Hendzel, PhD for their contribution in preparing patients for image acquisition.

ABBREVIATIONS

| | |
|-------|--|
| MI | Myocardial Infarction |
| MRI | Magnetic Resonance Imaging |
| SPECT | Single Photon Emission Computed Tomography |
| CAD | Coronary Artery Disease |
| DE | Delayed enhancement |
| MIV | MIBI In Volume (perfusion index in numbers of counts per volume in cm ³) |
| VOI | Volume Of Interest |

REFERENCES

- Heusch G. Hibernating Myocardium. *Physiological Reviews* 1998;78:1055–85.
- Allman KC, Shaw LJ, Hachamovitch R, Udelson JE. Myocardial viability testing and impact of revascularization on prognosis in patients with coronary artery disease and left ventricular dysfunction: a meta-analysis. *J Am Coll Cardiol* 2002;39:1151–8.
- Pasquet A, Robert A, D'Hondt AM, Dion R, Melin JA, Vanoverschelde JL. Prognostic value of myocardial ischemia and viability in patients with chronic left ventricular ischemic dysfunction. *Circulation* 1999;100:141–8.
- Sharir T, Germano G, Kang X, Lewin HC, Miranda R, Cohen I, Agafitei RD, Friedman JD, Berman DS. Prediction of Myocardial Infarction Versus Cardiac Death by Gated Myocardial Perfusion SPECT: Risk Stratification by the Amount of Stress-Induced Ischemia and the Poststress Ejection Fraction. *J of Nucl Med* 2001;42:831–7.
- Wilson JM. Reversible congestive heart failure caused by myocardial hibernation. *Tex Heart Inst J* 1999;26:19–27.
- Rahimtoola SH. A perspective on the three large multicenter randomized clinical trials of coronary bypass surgery for chronic stable angina. *Circulation* 1985;72:V-123–35.
- Brown TA. Hibernating myocardium. *Am J Crit Care* 2001;10:84–91.
- Soman P, Udelson AJ. Prognostic and therapeutic implications of myocardial viability in patients with heart failure. *Curr Cardiol Rep* 2004;6:211–6.
- Elsasser A, Schlepper M, Klovekorn WP, Cai WJ, Zimmermann R, Muller KD, Strasser R, Kostin S, Gagel C, Munkel B, Schaper W, Schaper J. Hibernating myocardium: an incomplete adaptation to ischemia. *Circulation* 1997;96:2920–31.
- Gunning MG, Kaprielian RR, Pepper J, Pennell DJ, Sheppard MN, Severs NJ, Fox KM, Underwood R. The histology of viable and hibernating myocardium in relation to imaging characteristics. *J Am Coll Cardiol* 2002;39:428–35.
- Gerber BL, Garot J, Bluemke DA, Wu KC, Lima JA. Accuracy of contrast-enhanced magnetic resonance imaging in predicting improvement of regional myocardial function in patients after acute myocardial infarction. *Circulation* 2002;106:1083–9.
- Soto JR, Beller GA. Clinical benefit of noninvasive viability studies of patients with severe ischemic left ventricular dysfunction. *Clin Cardiol* 2001;24:428–34.
- Watzinger N, Saeed M, Wendland MF, Akbari H, Lund G, Higgins CB. Myocardial viability: magnetic resonance assessment of functional reserve and tissue characterization. *J Cardiovasc Magn Reson* 2001;3:195–208.
- Kim RJ, Shah DJ, Judd RM. How we perform delayed enhancement imaging. *J Cardiovasc Magn Reson* 2003;5:505–14.
- Kuhl HP, Beek AM, van der Weerd AP, Hofman MBM, Visser CA, Lammertsma AA, Heussen N, Visser FC, van Rossum AC. Myocardial viability in chronic ischemic heart disease—comparison of contrast-enhanced magnetic resonance imaging with 18F-fluorodeoxyglucose positron emission tomography. *J Am Coll Cardiol* 2003;41:1341–8.
- Klein C, Nekolla SG, Bengel FM, Momose M, Sammer A, Haas F, Schnackenburg B, Delius W, Mudra H, Wolfram D, Schwaiger M. Assessment of myocardial viability with contrast-enhanced magnetic resonance imaging—comparison with positron emission tomography. *Circulation* 2002;105:162–7.
- Kim RJ, Fieno DS, Parrish TB, Harris K, Chen EL, Simonetti O, Bundy J, Finn JP, Klocke FJ, Judd RM. Relationship of MRI delayed contrast enhancement to irreversible injury, infarct age, and contractile function. *Circulation* 1999;100:1992–2002.
- Kim RJ, Wu E, Rafael A, Chen EL, Parker MA, Simonetti O, Klocke FJ, Bonow RO, Judd RM. The use of contrast-enhanced magnetic resonance imaging to identify reversible myocardial dysfunction. *N Engl J Med* 2000;343:1445–53.
- Schwartzman PR, Srichai MB, Grimm RA, Obuchowski NA, Hammer DF, McCarthy PM, Kasper JM, White RD. Nonstress delayed-enhancement magnetic resonance imaging of the myocardium predicts improvement of function after revascularization for chronic ischemic heart disease with left ventricular dysfunction. *Am Heart J* 2003;146:535–40.
- Choi KM, Kim RJ, Gubernikoff G, Vargas JD, Parker M, Judd RM. Transmural extent of acute myocardial infarction predicts long-term improvement in contractile function. *Circulation* 2001;104:1101–7.
- Gerber BL, Garot J, Bluemke DA, Wu KC, Lima JAC. Accuracy of contrast-enhanced magnetic resonance imaging in predicting improvement of regional myocardial function in patients after acute myocardial infarction. *Circulation* 2002;106:1083–9.
- Shan K, Constantine G, Sivanathan M, Flamm SD. Role of cardiac magnetic resonance imaging in the assessment of myocardial viability. *Circulation* 2004;109:1328–34.
- Hillenbrand HB, Kim RJ, Parker MA, Fieno DS, Judd RM. Early assessment of myocardial salvage by contrast-enhanced magnetic resonance imaging. *Circulation* 2000;102:1678–83.
- Wu E, Judd RM, Vargas JD, Klocke FJ, Bonow RO, Kim RJ. Visualization of presence, location, and transmural extent of healed Q-wave and non-Q-wave myocardial infarction. *Lancet* 2001;357:21–8.
- Kim RJ, Judd RM. Fundamental concepts in myocardial viability assessment revisited: when knowing how much is “alive” is not enough. *Heart* 2004;90:137–40.
- Kim RJ, Hillenbrand HB, Judd RM. Evaluation of myocardial viability by MRI. *Herz* 2000;25:417–30.
- Wagner A, Mahrholdt H, Holly TA, Elliott MD, Regenfus M, Parker M, Klocke FJ, Bonow RO, Kim RJ. Contrast-enhanced MRI and routine single photon emission computed tomography (SPECT) perfusion imaging for detection of subendocardial myocardial infarcts: an imaging study. *Lancet* 2003;361:374–9.
- Gunning MG, Anagnostopoulos C, Knight CJ, Pepper J, Burman ED, Davies G, Fox KM, Pennell DJ, Underwood SR. Comparison of thallium-201, technetium-99m-tetrofosmin and dobutamine magnetic resonance imaging for identifying hibernating myocardium. *Circulation* 1998;98:1869–74.
- Gibbons RJ, Miller TD, Christian TF. Infarct size measured by SPECT imaging with 99mTc-Sestamibi—a measure of the efficacy of therapy in acute myocardial infarction. *Circulation* 2000;101:101–8.

30. Cuocolo A, Acampa W, Nicolai E, Pace L, Petretta M, Salvatore M. Quantitative thallium-201 and technetium 99m sestamibi tomography at rest in detection myocardial viability in patients with chronic ischemic left ventricular dysfunction. *J Nucl Cardiol* 2000;7:8–15.
31. Murashita T, Makino Y, Kamikubo Y, Yasuda K, Mabuchi M, Tamaki N. J Quantitative gated myocardial perfusion single photon emission computed tomography improves the prediction of regional functional recovery in akinetic areas after coronary bypass surgery: useful tool for evaluation of myocardial viability. *Thorac Cardiovasc Surg* 2003;126:1328–34.
32. Ross J. Myocardial perfusion-contraction matching. Implications for coronary heart disease and hibernation *Circulation* 1983;107:6–83.
33. Schmidt M, Voth E, Schneider CA, Theissen P, Wagner R, Baer FM, Schicha H. F-18-FDG uptake is a reliable predictor of functional recovery of akinetic but viable infarct regions as defined by magnetic resonance imaging before and after revascularization. *Magn Reson Imaging* 2004;22:229–36.
34. Rehwald WG, Fieno DS, Chen EL, Kim RJ, Judd RM. Myocardial magnetic resonance imaging contrast agent concentration after reversible and irreversible ischemic injury. *Circulation* 2002;105:224–9.
35. Slomka PJ. Software approach to merging molecular with anatomic information. *J Nucl Med* 2004;45 Suppl1:36S–45S.
36. Aladi UE, Hurwitz GA, Dey D, Levin D, Drangova M, Slomka PJ. Automated image registration of gated cardiac single-photon emission computed tomography and magnetic resonance imaging. *J Magn Reson Imaging* 2004;19(3):283–90.
37. Miller TD, Christian TE, Hopfenspringer MR, Hodge DO, Gersh BJ, Gibbons RJ. Infarct size after acute myocardial infarction measured by quantitative tomographic 99mTc sestamibi imaging predicts subsequent mortality. *Circulation* 1995;92:334–41.
38. Hurrell DG, Milavetz J, Hodge DO, Gibbons RJ. Infarct size determination by technetium 99m sestamibi single-photon emission computed tomography predicts survival in patients with chronic coronary artery disease. *Am Heart J* 2000;140:61–6.
39. Fieno DS, Kim RJ, Chen EL, Lomansney JW., Klocke FJ, Judd RM. Contrast—enhanced magnetic resonance imaging of myocardium at risk: Distinction between reversible and irreversible injury throughout infarct healing. *J Am Coll Cardiol* 2000;36:1985–91.